NUMERICAL AND EXPERIMENTAL INVESTIGATION ON TURBULENCE STRUCTURES IN A DRAG-REDUCING FLOW WITH SURFACTANT ADDITIVES

Bo Yu[1,2] , Fengchen Li[1,2] and Yasuo Kawaguchi[1*],
1. Turbomachinery Research Group,
Institute for Energy Utilization,
National Institute of Advanced Industrial Science and Technology,
1-2 Namiki, Tsukuba, Ibaraki 305-8564, Japan
2. Center for Smart Control of Turbulence
yuu-bo@aist.go.jp, lifch-ri@aist.go.jp, kawaguchi.y@aist.go.jp

ABSTRACT

DNSs and experiments were carried out for a turbulent channel flow of a 75 ppm CTAC (Cetyltrimethyl ammonium chloride) surfactant solution. The numerical and experimental results such as velocity profiles, root-mean-square velocity fluctuations, Reynolds shear stress, and production of turbulent kinetic energy were compared. The results were also compared with those of Newtonian fluid flow at similar Reynolds numbers.

INTRODUCTION

More than 50 years have passed since Toms (1948) discovered that the addition of a minute amount of long-chain polymer into liquid such as water can reduce turbulent friction drag significantly. Thought huge experiments have been performed to investigate the drag-reducing flow, the mechanism of the drag-reduction has not been satisfactorily discovered. The first theoretical explanation was proposed by Lumley (1969), who postulated that the increased extensional viscosity due to the stretching of randomly coiled polymers trends to damp the small eddies in the buffer layer, thicken the buffer layer, and consequently result in the drag-reduction. In the meanwhile, Lumley stressed that drag-reduction occurs only when the relaxation time of the solution is larger than the characteristic time scale of the turbulence flow. Another important theory was proposed by De Gennes (1990), who criticized the scenario by using extensional viscosity and argued that the elastic energy stored in the macromolecules causes drag-reduction. However, these explanations are qualitatively. Recently DNS has been used to analyze the turbulence transport mechanism. One of its super advantages is that the instantaneous flow structures near the wall can be calculated accurately, which are quite difficult to be precisely measured in experiments. Especially the instantaneous extra stress associated with the deformation of macromolecules can be calculated which appears not be measured by experiments yet. These quantitative data are helpful in analyzing the mechanism of drag-reduction. Another advantage is that the effects of various physical properties can be easily isolated and studied in comparison with experiments. Some main conclusions of the previous DNSs on the drag-reducing flow by additives are summarized below. Orlandi (1995) and Den Toonder et al. (1997) carried out DNS by using extensional viscosity models for a channel and a pipe flow respectively, and their results qualitatively agree with most of the experimental observations. However, the inelastic characteristic of such extensional models cannot examine the onset phenomenon. Sureshkumar et al. (1997) performed direct numerical simulations for a fully developed turbulence channel flow by using a viscoelastic FENE-P model, based on which they verified Lumley's hypothesis that drag-reduction is primarily an effect of the extension of the polymer chains where the increase in the extensional viscosity leads to the inhibition of turbulence generating events, and proposed a criterion for the onset of the drag-reduction. Angelis et al. (2002) further confirmed the ability of FENE-P model to reproduce most of the essential effects of polymers in dilute solution on the wall turbulence. Min et al. (2001) studied the role of elastic energy in turbulence drag-reduction by polymer additives using an Oldroyd-B model. Yu et al. (2003) studied the effect of Weissenberg number on the turbulence flow structure with a Giesekus model. In all the above studies using viscoelastic models (Sureshkumar et al. (1997); Angelis et al. (2002); Min et al. (2001) and Yu et al. (2003)), the parameters in the constitutive equations are set artificially, hence the comparisons of the numerical and experimental results are not correspondingly. Suzuki et al. (2001) attempted to use the model parameters well fitted the apparent shear viscosities for the calculations of the drag-reducing flow of surfactant solution, but they found no drag-reduction. In the present study, we carried out both experimental and numerical studies for a turbulent channel flow of the 75 ppm CTAC solution. A Giesekus constitutive equation was used to calculate the extra stress due to the surfactant additives and the model parameters were obtained by well fitting the measured shear viscosities of the 75 ppm CTAC surfactant solution. We wish to compare the numerical results with the experimental data to clarify the mechanism of turbulence transport in the drag-reduction flow by surfactant additives.

EXPERIMENTAL

Figure 1 schematically shows the closed loop flow facility used in the present experiment, in which the pump drives the fluids pass through the storage tank, the contraction with a filter, the test channel and diffuser in circulation. The channel is 0.04 m high, 0.5m wide and 10 m long (inside measurement). To remove large eddies, a honeycomb was employed at the entrance of the test section.

Table 1 Computational parameters

	Re_τ	Re_m	We_τ	β	α	$L_x \times L_y \times L_z$	$N_x \times N_y \times N_z$	Δx^+	Δy^+	Δz^+
Surfactant	300	12080	54	4	0.005	$10h \times 2h \times 5h$	96×128×96	31.3	0.4~9	15.6
Newtonian	380	13070	×	0	×	$3h \times 2h \times 1.5h$	128×128×128	8.9	0.5~11	4.5

Table 2 Friction factor and drag-reduction rate

		Re_m	C_f	C_f^*	C_f^{**}	DR %
Numerical	surfactant solution	12080	0.00493	0.00696	0.00248	29%
	Newtonian fluid	13070	0.00683	0.00676	×	×
Experimental	surfactant solution	12400	0.00310	0.00692	0.00245	53%
	Newtonian fluid	12400	0.00659	0.00692	×	×

The flow rate and the pressure drop were measured by an electromagnetic flow meter with uncertainty of $1.67\times10^{-4} m^3/s$ and a precise pressure gage respectively. The velocity components in both the streamwise and wall-normal directions were measured with a two-component LDV system using 488 and 514.5 nm wavelength of light. The LDV measurement position was 9 m downstream from the inlet of the test section and the measurements were made from the wall surface to a position of 0.01 m away from the wall (a quarter of the channel height) at the middle vertical x-y plane of the channel.

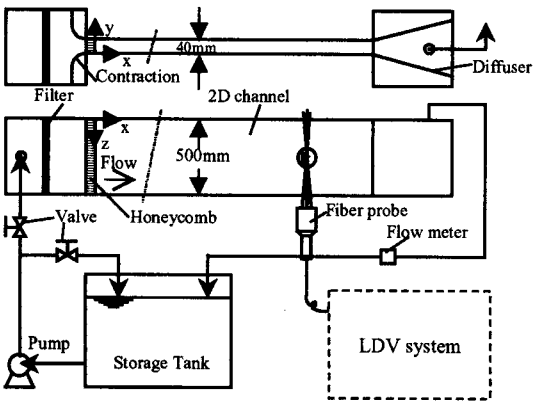

Figure 1 Schematic diagram of the fluid Loop

The surfactant solution used in the present study was cetyltrimethyl ammonium chloride (CTAC) dissolved in tap water with a concentration 75ppm. The sodium salicylate was added to the solution to provide counter-ions with a weight concentration the same as that of CTAC. Experimental measurement was carried out at a constant temperature 30 °C. The measured mean Reynolds number Re_m was 12400. For comparison measurements were carried out for Newtonian fluid flow (water) at the same Reynolds number.

NUMERICAL PROCEDURE

We measured both the shear viscosities and extensional viscosities of the CTAC surfactant solution and found that the Giesekus model can qualitatively describe our measured shear viscosities and extensional viscosities (Kawaguchi et al., 2003). The measured extensional viscosities are not sufficient accurate to permit the determination of the numerical values of constitutive parameters. For this reason the parameters in the constitutive equation (Eq.(3) below) were determined by fitting the reliable shear viscosity data. Figure 2 shows the shear viscosities of the 75 ppm CTAC surfactant solution versus shear rates at temperature 30°C which are well fitted by the curve of Giesekus model with the parameters listed in the figure. DNSs were carried out for a fully developed turbulence channel flow by employing the Giesekus model with the constitutive parameters determined above. The dimensionless governing equations for the fully developed turbulence channel flow of the CTAC surfactant solution can be written as:

Continuity equation:

$$\frac{\partial u_i^+}{\partial x_i^*} = 0 \tag{1}$$

Momentum equation:

$$\frac{\partial u_i^+}{\partial t^*} + u_j^+ \frac{\partial u_i^+}{\partial x_j^*} = -\frac{\partial p^+}{\partial x_i^*} + \frac{1}{Re_\tau}\frac{\partial}{\partial x_j^*}\left(\frac{\partial u_i^+}{\partial x_j^*}\right) + \frac{\beta}{We_\tau}\frac{\partial c_{ij}^+}{\partial x_j^*} + \delta_{1i} \tag{2}$$

Constitutive equation:

$$\frac{\partial c_{ij}^+}{\partial t^*} + \frac{\partial u_m^+ c_{ij}^+}{\partial x_m^*} - \frac{\partial u_i^+}{\partial x_m^*} c_{mj}^+ - \frac{\partial u_j^+}{\partial x_m^*} c_{mi}^+ + \frac{Re_\tau}{We_\tau}\left[c_{ij}^+ - \delta_{ij} + \alpha\left(c_{im}^+ - \delta_{im}\right)\left(c_{mj}^+ - \delta_{mj}\right)\right] = 0 \tag{3}$$

c_{ij}^+ is the conformation component. β is defined as $\beta = \eta_a / \eta_s$, where η_a and η_s are surfactant contribution and solvent contribution to the zero-shear rate viscosity of the solution ($\eta_0 = \eta_a + \eta_s$) respectively. The Reynolds number

and Weissenberg number are defined as: $\mathrm{Re}_\tau = \rho u_\tau h/\eta_s$ and $\mathrm{We}_\tau = \rho\lambda u_\tau^2/\eta_s$, where ρ, λ, u_τ and h are the fluid density, the relaxation time, the friction velocity and half the channel height respectively. Note that the Reynolds number and Weissenberg number are based on the viscosity of solvent. By setting $\beta = 0$, the Navier-stokes equation for Newtonian fluid is recovered. For comparison, a DNS was carried out for Newtonian fluid.

The boundary conditions are referred to Yu et al. (2003). For spatial discretization, a second-order finite difference scheme was employed with MINMOD scheme discretizing the convective term in the constitutive equation (Yu et al. 2003). Table 1 lists the computational parameters for both the surfactant solution and Newtonian fluid. For the surfactant solution, a larger computational domain was employed due to the relaxation time and a coarser mesh was used owing to larger eddy sizes in the drag-reducing flow.

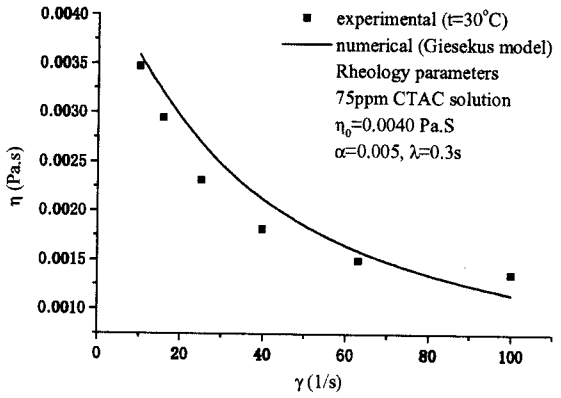

Figure 2 Shear viscosity versus shear rate

RESULTS

The drag-reduction rate by surfactant additives with respect to Newtonian fluid is defined as the reduction of friction factor at equal mean Reynolds number Re_m for the Newtonian fluid and surfactant solution. In the experiments the mean Reynolds numbers were well adjusted the same for surfactant solution and Newtonian fluid (water) to Re_m=12400. For the numerical simulation, the mean Reynolds numbers for the surfactant solution and Newtonian fluid are slightly different from Re_m=12400 as shown in Table 2. We could adjust Re_τ slightly to satisfy Re_m=12400, but it is not necessary because the small variations of the Reynolds number only alter turbulence characteristics such as friction factor, root-mean square velocity fluctuations and Reynolds shear stress slightly. Table 2 shows that the measured and calculated friction factors of the Newtonian fluid are in good agreement with the Dean's equation. In Table2, C_f^* was evaluated by Dean's correlation (Dean,1978) and C_f^{**} by the limited friction factor asymptote (Virk et al., 1970). The measured drag-reduction rate of the surfactant solution is 53%, which is larger than the predicted value of 29%. Both the numerical and the experimental friction factors for surfactant solution are larger than Virk's asymptotic friction factor (Virk et al., 1970).

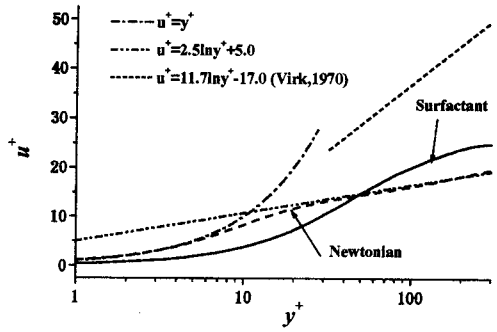

(a) numerical

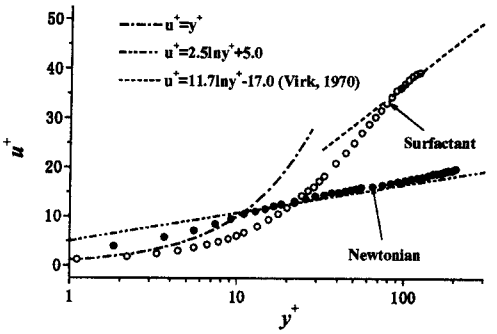

(b) experimental

Figure 3 Velocity profiles

Figure 3 compares the mean streamwise velocity profiles of the fully developed turbulence flow of Newtonian fluid and CTAC surfactant solution, in which the well-known relationships of Newtonian fluids — linear law in the viscous sublayer $u^+ = y^+$ and logarithmic law $u^+ = 2.5\ln y^+ + 5.0$ in the inner layer, and Virk's asymptote velocity profile for the drag-reducing flow are given for comparison. The numerical results shown in Fig. 3(a) qualitatively agree with the experimental data in Fig. 3(b): in the viscous sublayer the velocity values of the surfactant solution are smaller than those of Newtonian fluid and in the logarithmic layer the velocity profile of surfactant solution is upshifted as compared to Newtonian fluid. The numerical velocity profile of the Newtonian fluid collapses to $u^+ = y^+$ in the viscous sublayer and slightly lower than $u^+ = 2.5\ln y^+ + 5.0$ in the logarithmic layer as shown in Fig. 3(a). The larger values of the velocities in the viscous sublayer measured by the LDV are most probably due to the interaction between the measured volume and the wall surface. In the logarithmic region the measured values agree well with the logarithmic law. Both Fig. 3 (a) and 3(b) show that the addition of surfactant additives dramatically lower the velocity values in the viscous sublayer. It is interesting to note that the velocity profile of surfactant solution in Fig. 3(b) approaches more to the Virk's asymptote velocity profile as compared to that in Fig. 3(a), which is corresponding to a higher drag-reduction rate.

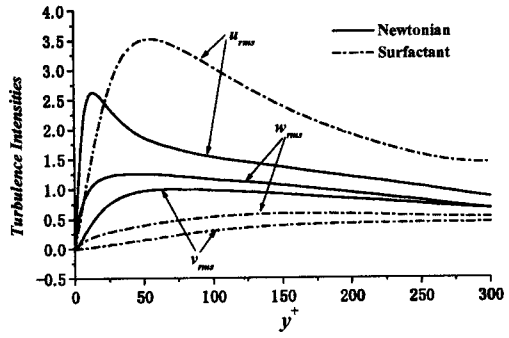

(a) numerical

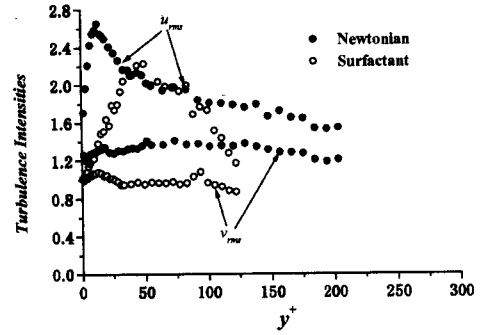

(b) experimental

Figure 4 Root-mean- square velocity fluctuations

The root-mean-square velocity fluctuations obtained in numerical simulations and experiments are presented in Fig. 4 (a) and (b) respectively. In Fig. 4(b), only two components u^+_{rms} and v^+_{rms} are given because our LDV measurement is two-dimensional. Both the numerical and experimental results show that as compared to Newtonian fluid the location where the u^+_{rms} reaches its maximum value shifts from the wall region to the bulk flow and the v^+_{rms} decreases appreciably for the surfactant solution. The experiment shows that the addition of surfactant additives makes the maximum value of the u^+_{rms} decrease while the numerical simulation shows an increase. But for larger Reynolds numbers such as $\mathrm{Re}_m = 3\times10^4$, our experiments show that the peak value is larger than that of Newtonian flow. A decrease of w^+_{rms} by adding surfactant additives is seen in Fig.4 (a). The decrease of the velocity fluctuation intensities in the wall-normal and spanwise directions is because of the energy redistribution as shown later.

Figure 5(a) shows that by adding surfactant additives the viscous shear stress increases appreciably except in the vicinity of the wall, the Reynolds shear stress decreases dramatically with its maximum value around half that of Newtonian fluid, and the location where Reynolds shear stress reaches its maximum value shifts from the wall region to the bulk flow. The decrease of the Reynolds shear stress for the drag-reducing flow is owing to the increase of the viscous shear stress and the positive contribution of the viscoelastic shear stress, primarily the latter. Note that the viscoelastic stress defined by $\beta c^+_{xy}/\mathrm{We}_\tau$ is the largest component in the near wall region among all the stress components, and it is about 50 percentage of the total shear stress in the whole region of the channel. The decrease of the Reynolds shear stress was observed in the experiments as shown in Fig.5(b), and the measured Reynolds shear stresses are smaller than those predicted.

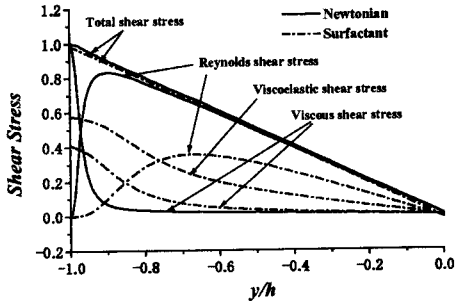

(a) numerical

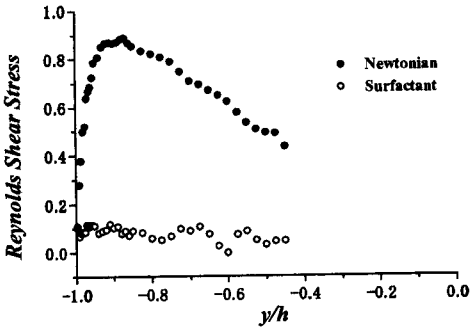

(b) experimental

Figure 5 Shear stress

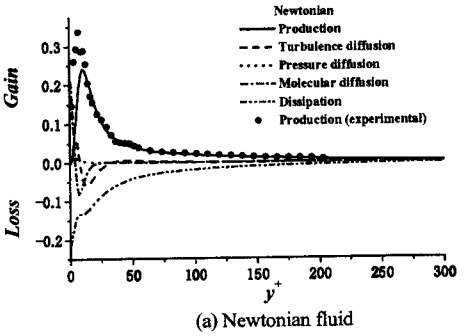

(a) Newtonian fluid

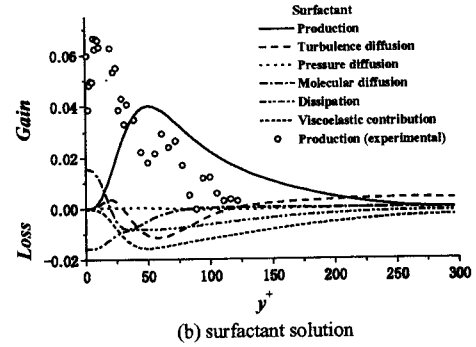

(b) surfactant solution

Figure 6 Budget of turbulent kinetic energy

The Budget terms of Reynolds stress $\overline{u_i^{+} u_j^{+}}$ can be expressed as

$$\frac{D}{Dt}\left(\overline{u_i^{+} u_j^{+}}\right) = P_{ij} + T_{ij} + D_{ij} + \Pi_{ij} - \varepsilon_{ij} + E_{ij} \qquad (4)$$

where $P_{ij}, T_{ij}, D_{ij}, \Pi_{ij}, \varepsilon_{ij}$ and E_{ij} are the production, turbulence transportation, molecular diffusion, velocity-pressure gradient correlation, dissipation rate and elastic contribution term respectively. The elastic contribution term can be written as:

$$E_{ij} = \frac{\beta}{\mathrm{We}_\tau}\left(\overline{u_i'^+ \frac{\partial c_{jk}'^+}{\partial x_k^+}} + \overline{u_j'^+ \frac{\partial c_{ik}'^+}{\partial x_k^+}}\right) \quad (5)$$

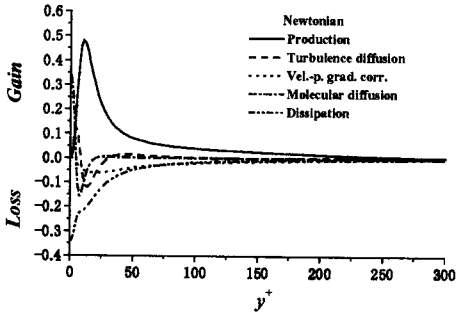

(a) Newtonian fluid

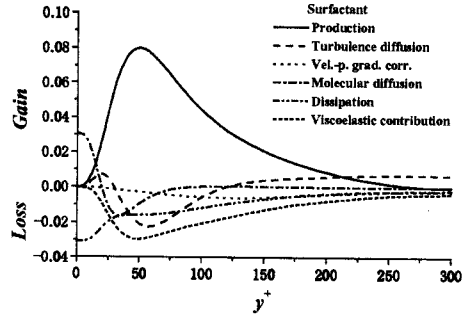

(b) surfactant solution

Figure 7 Budget of Reynolds stress $\overline{u'^+u'^+}$

The turbulent kinetic energy budget is obtained by setting $i = j$, summing over the index i in Eq. 4 and dividing the summation by 2. The budget terms of the turbulent kinetic energy are plotted in Fig.6 as a function of dimensionless wall distance y^+ for both the Newtonian fluid and the CTAC surfactant solution. The production rates calculated by the measured instantaneous velocity fluctuations are also included for comparison. It is seen clearly that the absolute value of budget terms decrease significantly by the addition of surfactant additives. The peak values of various turbulence quantities, for instant production, decrease dramatically. The percentage decrease of the dissipation term is around 93%, which is larger than that of production around 83% (the percentage decrease is estimated by the variation of peak value as compared to Newtonian fluid). The larger decrease percentage of the dissipation rate is because the viscoelastic contribution acts as a strong sink term along the channel height, in fact except in the near wall region, the viscoelastic contribution is the largest loss term. The locations where production reaches its maximum value, molecular diffusion and turbulence diffusion attain their minimum values are shifted from wall region to the bulk flow region, for example, the location shifts from $y^+ = 10$ to 50 for production rate. These shifts are consistent with the expansion of the buffer layer. It is interesting to note that the negative peak position of the viscoelastic contribution is the almost the same as that of production rate, which shows the action of the surfactant additives on turbulence flow is primarily in the buffer layer. Though the surfactant additives changes the values and distribution of the budget terms significantly, the production, turbulent diffusion, molecular diffusion and other terms show identical variation trend between Newtonian and surfactant solution, with the latter varying flatly. The measured production rates of the Newtonian fluid agree well with the numerical predictions except in the near wall region, at which the experimental values are larger. The agreement of the production rates of the CTAC surfactant solution between experiment and numerical calculation is qualitatively good. The measured peak value is larger and its location shifts less further to the bulk flow than the numerical peak does.

The budget terms of the normal components of Reynolds normal stress $\overline{u'^+u'^+}$, $\overline{v'^+v'^+}$ and $\overline{w'^+w'^+}$ are shown in Fig.7-9 respectively. As compared to Newtonian fluid, the magnitude of all the budget terms become smaller and the peak value positions move toward the center of the channel for the surfactant solution. The magnitude of the budget terms of $\overline{v'^+v'^+}$ and $\overline{w'^+w'^+}$ are much smaller than those of $\overline{u'^+u'^+}$ for both Newtonian fluid and surfactant solution. The decrease amplitudes of the budget terms of $\overline{v'^+v'^+}$ and $\overline{w'^+w'^+}$ are larger than those of $\overline{u'^+u'^+}$. The production rate of $\overline{u'^+u'^+}$ is twice the production rate of the turbulent kinetic energy because the production rates are zero for the normal component $\overline{v'^+v'^+}$ and spanwise component $\overline{w'^+w'^+}$. It is well known that the pressure strain term $\overline{p'\partial u_i'^+/\partial x_i^+}$ plays a dominant role on energy redistribution over the three normal components of Reynolds normal stress and due to continuity $\sum \overline{p'\partial u_i'^+/\partial x_i^+} = 0$ must be satisfied. It is clearly seen in Fig.7 that the by the addition of surfactant additives the magnitude of the pressure strain becomes significantly smaller, which means as compared to Newtonian fluid the energy transferred from the streamwise component to the other two components becomes much smaller. Figures 8 and 9 show that normal and spanwise velocity-pressure gradient correlations (they are usually considered as pseudo-productions because they have positive values) of the surfactant solution are less than one tenth of the values of Newtonian fluid. This is the reason why v_{rms}^+ and w_{rms}^+ of the surfactant solution decrease significantly as compared to Newtonian fluid. The change of the budget terms of the Reynolds normal stress $\overline{v'^+v'^+}$ and $\overline{w'^+w'^+}$ are flat, which explains the flat distribution of the v_{rms}^+ and w_{rms}^+ along the channel height as shown in Fg.4. The turbulent diffusion of $\overline{v'^+v'^+}$ of the surfactant solution becomes negligible, which indicates that the turbulent transportation in normal direction becomes very weak with the addition of the additives. In the Newtonian fluid, the dissipation terms almost balance the velocity-pressure gradient terms in the budget of $\overline{v'^+v'^+}$ and $\overline{w'^+w'^+}$. However, with the addition of surfactant additives, the dissipation term becomes very small and a viscoelastic term due to the relaxation becomes a dominant dissipation term which balance the velocity-pressure gradient term. This shows that viscoelasticity plays an important role in the redistribution of the budget of the Reynolds stress.

CONCLUSION

DNSs and experiments were performed for the fully developed turbulence flow of Newtonian fluid and 75ppm CTAC surfactant solution in a channel. A Giesekus model

was chosen because it can well describe the Rheological properties of the CTAC surfactant solution. The numerical and experimental studies show that:

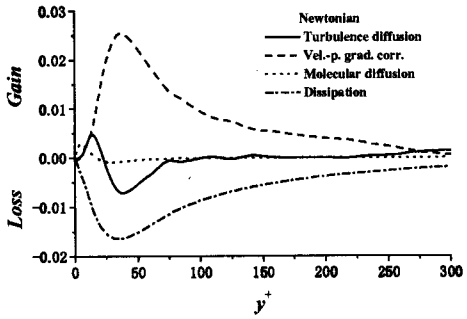

(a) Newtonian fluid

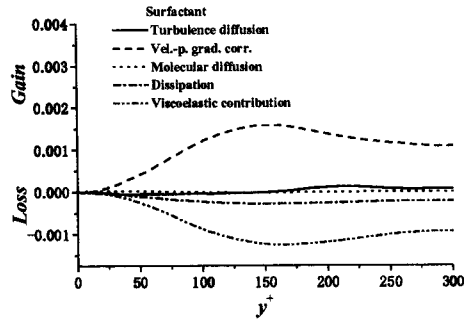

(b) surfactant solution

Figure 8 Budget of Reynolds stress $\overline{v^+v^+}$

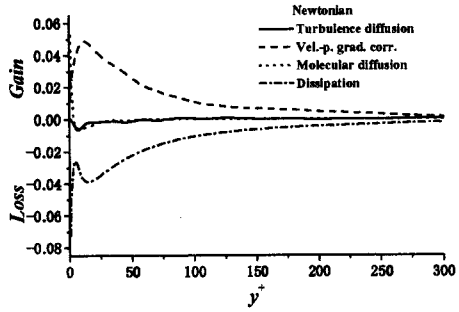

(a) Newtonian fluid

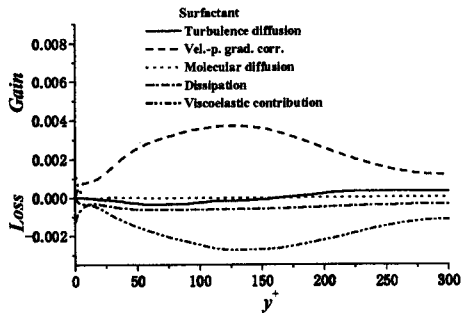

(b) surfactant solution

Figure 9 Budget of Reynolds stress $\overline{w^+w^+}$

(1) the addition of surfactant additives into the fully developed turbulence water flow in a channel alters the mean streamwise velocity profile — the buffer layer is expanded, u^+ is appreciably smaller than y^+ in the viscous sublayer and the slope of the velocity profile in the logarithmic layer increases in comparison with Newtonian fluid;

(2) the root-mean-square velocity fluctuations in the wall normal direction decrease for the drag-reducing flow;

(3) the locations where u^+_{rms} and Reynolds shear stress attain their maximum value are shifted from the wall region to the bulk flow region by adding surfactant additives;

(4) the measured peak streamwise velocity fluctuation intensity shows a decrease while numerical peak shows an increase as compared to Newtonian flow (this discrepancy indicates that the model parameters need to be determined in more confident method or more suitable model should be adopted/ developed for the surfactant solution);

(5) the Reynolds shear stress decreases dramatically and the deficit of the Reynolds shear stress is mainly compensated by the viscoelastic shear stress;

(6) the normal and spanwise velocity-pressure gradient correlations are significantly reduced, which explain the decrease of v^+_{rms} and w^+_{rms};

(7) the magnitudes of all the budget terms of turbulent kinetic energy become much smaller and the locations where the peak value positions move toward the center of the channel by addition of surfactant additives. Viscoelasticity acts as a large loss term in the budget of the Reynolds stress.

ACKNOWLEDGEMENT

This study is supported by 'Ministry of Education, Culture, Sports, Science and Technology' through the project 'Smart Control of Turbulence: A Millennium Challenge for Innovative Thermal and Fluids System', Japan.

REFERENCE

Angelis E. De, Casciola C. M. and Piva R., 2002, *Computers & Fluids*, Vol.31, pp.495-507.

De Gennes P.G., 1990, "Introdution to Polymer Dynamics", Cambridge: Cambridge University Press.

Dean R.B., 1978, *Trans. ASME, Journal of Fluids Engineering*, Vol.100, pp.215-223.

DenToonder J.M.J., Hulsen M.A., Kuiken G.D.C. and Nieuwstadt F.T.M., 1997, *J. Fluid Mech.*, Vol.337, pp.193-231.

Kawaguchi Y., Wei J. J., Yu B. and Feng Z. P., 2003, Proc. Fluids Engineering Division Summer Meeting, July 6-11,2003, Honolulu, Hawaii.

Lumley J.L., 1969, *Ann. Rev. Fluid Mech.*, Vol. 1, pp.367-384.

Min T., Yoo J.Y., Choi H. and Joseph D.D., 2001, Proc. 2sd *Turbulence and Shear Flow Phenomena*, KTH, Stockholm, Vol. 3, pp.35-50.

Orlandi P., 1995, *J. Non-Newtonian Fluid Mechanics*, Vol.60, pp.277-301.

Sureshkumar R., Beris A.N. and Handler R. A., 1997, *Phys. Fluids*, Vol.9, pp.743-755.

Suzuki H., Ishihara K. and Usui H., 2001, In: Proc. 3rd Pacific Rim Conference on Rheology.

Toms B.A., 1948, Proc. 1st Int. Cong. Rheol., North Hollad, Amsterdam, Vol. 2, pp.135-141.

Virk P., Mickley H. and Smith K., 1970, *ASME J. Appl. Mech.*, Vol.37, pp.480-493.

Yu B. and Kawaguchi Y., 2003, *Int. J. Heat and Fluid Flow*, in press.